MAGNETIC SUSPENSION BASED FOURIER TRANSFORM INFRARED SPECTROMETER MECHANISM (FTIS)

I. Köker, EADS Astrium GmbH, *ingo.koeker@astrium.eads.net*
H. Langenbach, EADS Astrium GmbH, *harald.langenbach @astrium.eads.net*
M. Schmid, EADS Astrium GmbH, *manfred.schmid @astrium.eads.net*
J.M. Lautier, ESTEC, *jean-michel.lautier@esa.int*

Abstract

In the frame of an ESTEC technology contract the development of a Magnetically Suspended Fourier Transform Spectrometer Mechanism (FTIS) was carried out.
The aim of the development is to avoid the issues found in mechanically suspended systems and to provide an active alignment and disturbance rejection capability for spectrometer applications. In the frame of FTIS an actively controlled suspension system based on the use of magnetic bearings was defined, developed and built as a demonstration model.

1. INTRODUCTION

Fourier Transform Spectrometers (FTS) are widely in use today as remote sensing devices and have proven themselves in spaceborne applications for the purpose of surface studies of Earth and other planets. Such a device is e.g. the MIPAS (Michelson Interferometer for Passive Atmospheric Sounding) flying on ENVISAT and also built at Astrium GmbH.

Most of the interferometer scanning mechanisms flown up to now are based on conventional mechanical linear guidance systems and are suffering from the reproducible mechanical errors and from statistic bearing jitter during motion as well. In addition, they don't allow in flight realignment of the scanning mirror due to potential misalignments between the different equipment of the FTS. In order to avoid this major drawback and also the drawbacks introduced by tribology issues, the development of the technology of magnetic suspension for interferometer mechanisms is requested.

1.1. Technical Background

The technical principle dates back to the early 1800s when Michelson first invented the interferometer. Although modern systems include complex reference systems and filters, the basic device has remained essentially unchanged. Michelson's interferometer consisted of a half silvered mirror (beam splitter A) which divided a radiation source into two equal beams, a compensator plate (B) such that both beams would travel through the same length of optical material, one fixed mirror (D) and one moveable mirror (C) with which the two beams could be redirected to a common observer producing an interference pattern from which various properties of the radiation can be determined.

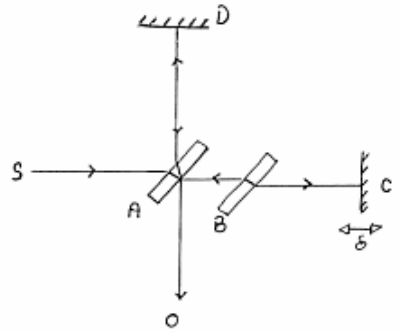

figure 1-1:Generic diagram of the Michelson Interferometer

Modern FTS devices make use of digital computing Fourier analysis and scanning devices to allow a rapid scan approach. In this approach, the optical path difference (δ) is varied in a continuous, linear manner with all scans beginning at $\delta = 0$.
The technology development performed is concerned with producing a mechanical linear guide for mirror C which will permit this path difference to be created and controlled. To achieve smooth motion and prolonged life, a non-contact guiding and control system consisting of a set of magnetic bearings and of the suitable closed loop controller is developed.

1.2. Initial Technical Requirements

Based on optical system inputs, an initial set of requirements was defined as a starting point for the mechanism development. The FTIS key requirements are as follows:

Requirement	Value
Linear stroke	200 mm
Speed	1 < Speed < 25 mm/sec
Speed stability	1%
Guidance Accuracy: - Mirror tilt max. - Tilt reproducibility - Lateral deviation - Lat. reproducibility	 5.0 µrad 0.3 µrad 50 µm 3 µm

Requirement	Value
Quasi static loads	+/- 45 g all axis

figure 1-2: Key Requirements for FTIS

It can be seen in figure 1-2 that the major performance critical requirements are related to tilt accuracy and reproducibility as well as to lateral reproducibility over stroke. These requirements were identified as the main design drivers during the development phase.

2. Design Concept

The design concept is shown in figure 3-1. A movable sled is constrained and controlled in 5 degrees of freedom (x, y, α, β, γ) by magnetic bearings. The 6th degree (z) will be controlled by use of a linear motor. The magnetic bearings F1y to F4y control the sled in lateral y direction and about the x and z-axis. The magnetic bearings F5x and F6x control the sled in lateral x direction and about the y-axis. The rotation axes are located between the magnetic bearings.

3. Design Features

3.1. Mechanical Design

The movable sled with the mounted mirror levitates between six magnetic bearings mounted to a base plate.

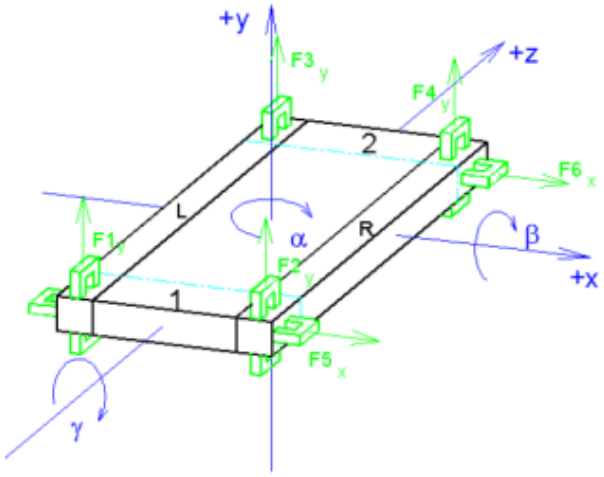

figure 3-1: magnetic bearing principle

The position of the sled in the magnetic bearing is measured via sensors against the rails in the sled. A linear motor drives the sled along its linear degree of freedom (z). An incremental linear encoder controls the position of the sled in z direction. End stops at both ends prevent the sled from leaving the travel range in case of a failure. During launch the sled is forced via four cup/cone interfaces attached to the four magnetic bearing brackets into its launch position.

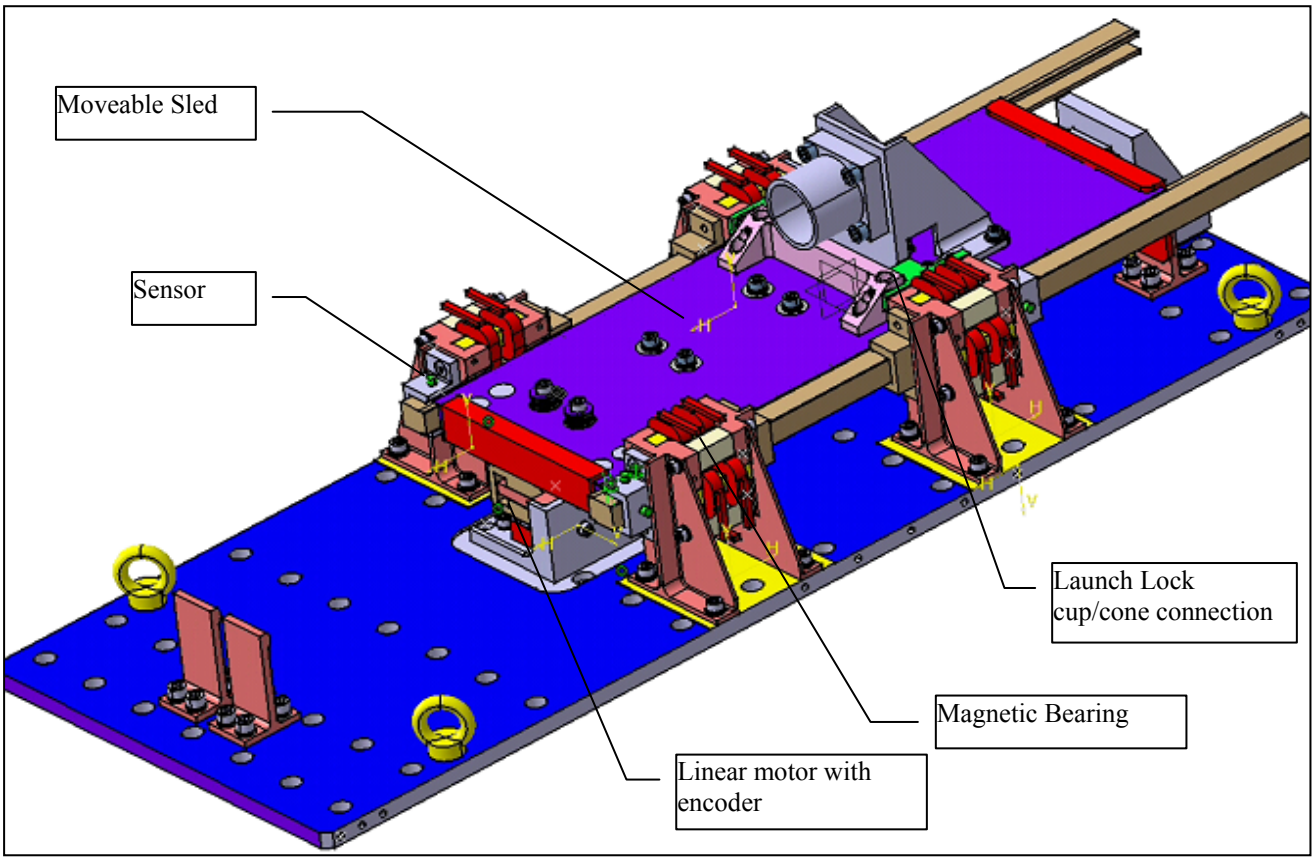

3.2. Active Magnetic Bearing (AMB)

A single AMB consists of two magnets acting in a pair in one actuation line producing a positive or negative force on the movable sled. One magnet consists of 2 coils with different polarity. One coil is constantly powered, producing the pre-magnetisation. The current of the other coil is controlled by the position controller.
The air gap of the magnetic bearing in nominal (centre) position at ambient temperature is 0.25 mm.

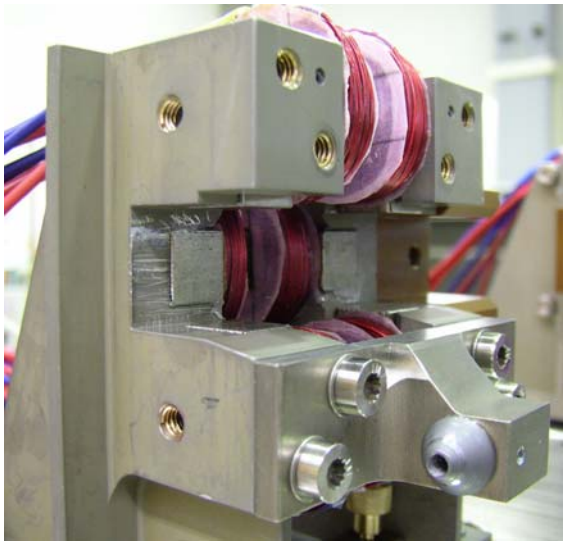

figure 3-2: Magnetic bearing pair

In figure 3-2 a magnetic bearing is shown for the vertical actuation direction and for the horizontal direction the part on the +x side is shown. Clearly visible are the 2 poles of the U-coil and the windings on them. Also the cup/cone connection for the Launch Lock is visible.

Due to the use of the differential windings (
figure 3-3) principle on the U-coils, an almost linear correlation between control current and magnetic force can be achieved.

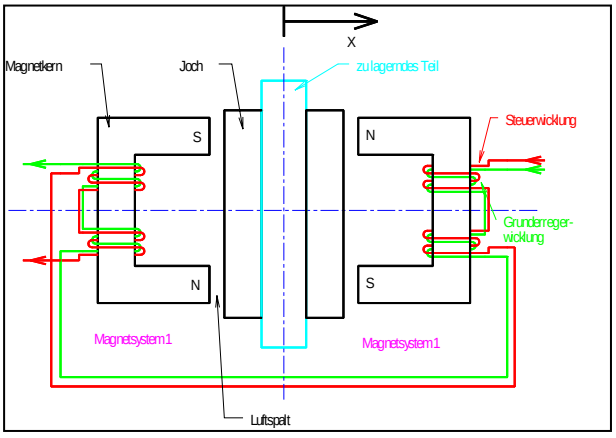

figure 3-3: differential winding principle

The slope of the characteristic curve and the maximum force can be varied by changing the main excitation current.

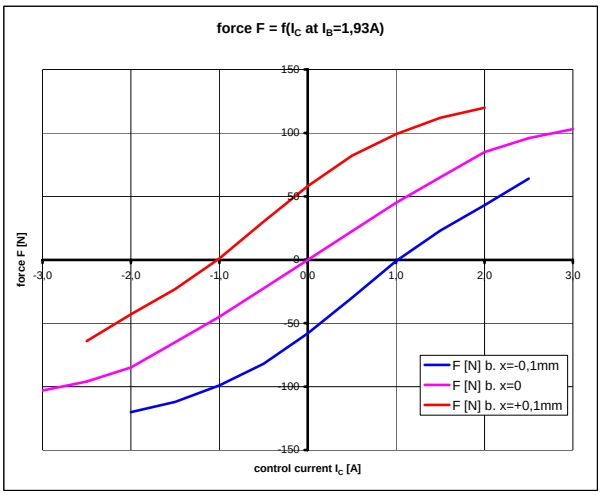

figure 3-4: force current characteristic

3.3. Position Sensor Principle

FTIS uses special eddy current sensors. This type of sensors shows an excellent resolution and signal to noise ratio.
As the target (rails) moves closer to one sensor, it moves away from the other. Therefore as the impedance in one leg of the inductive bridge increases, the other decreases. This push-pull effect amplifies the linear output-per-displacement and eliminates the need for summation amplifiers that would add noise and drift additionally into the system. As a result, differential systems provide greater resolution and thermal stability than single-ended systems.

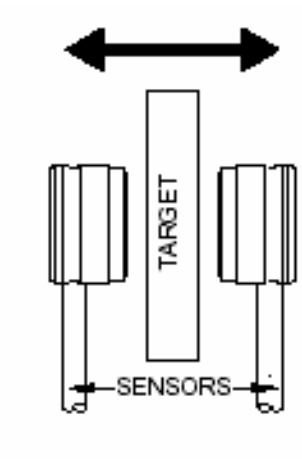

figure 3-5: sensor principle

The sensor resolution is about 0.4 µm. This resolution is sufficient to control the sled within the required accuracy.

Development test have been performed with the result that cross talk between the magnetic bearings and the sensors exists as the sensors are installed inside the U-coil. Therefore the eddy current sensors are placed outside the electro magnetic circuit hence not affected by the magnetic field of the bearing.

3.4. Controller Design

The controller design for the magnetic bearings is comprised of a 5-axis controller which controls the 5 degrees of freedom: x and y for the lateral directions and α, β and γ for the rotation about the 3 axes.

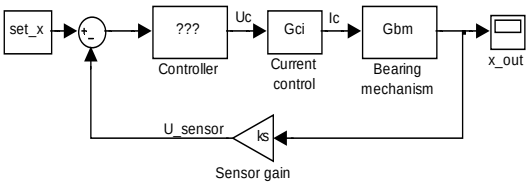

figure 3-6: magnetic bearing controller

The magnetic bearing is divided into an excitation coil and a control coil. The magnetic bearing control is performed by the control coils with a PID position controller. The excitation coil is powered with constant current. The transfer function of the PID controller is

$$G(p) = k_{R1}\left[k_{R2}\left(k_P + \frac{1}{p*T}\right) + \frac{p*T}{1+pT_1}\right] \qquad (1)$$

whereas 5 PID controllers are implemented into the complete set-up.

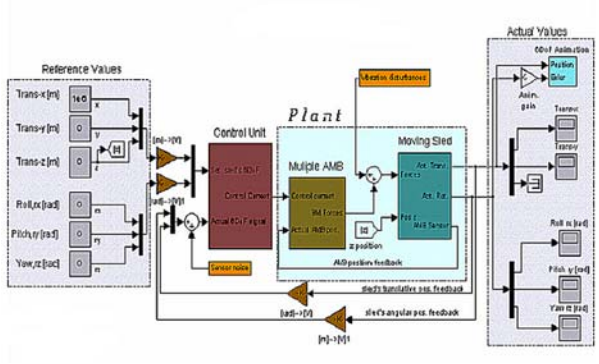

figure 3-7: model of position control loop

The signal from the 6 position sensor pairs are transformed compared with the required value, fed into the controller and back-converted for the generating of correct current values of the six magnetic bearings systems.

4. Development Test Results

4.1. Static Tests

During the commissioning phase of the magnetic bearings it became visible that the transfer factor for the used sensor did not match with the one from the manufacturer. The maximum range and the gain of the sensors system had to be readjusted. Finally the system was adjusted in static condition. One by one the magnetic bearing was set to operation until the system was levitated in all axes.
The parameters of the controller were adjusted such that the system was stable in all axes. Not only the stable system was a success criterion - also the start-up from a worst case position should be included. Even if the rails got attracted during the switch on of the excitation coils - it is possible to operate the system in a stable centre position after switching on the control coils.
Within this set-up the sled showed different eigenmodes in different z-positions.

Although designed for an excitation current of 1.93 A it was only possible to run the magnets with 1 A due to a design error in the choice of the amplifier piece parts. The potential drop over the bearing magnets was about 5.6 V; the remaining 22.4 V were dissipated in the amplifier of the control system which lead to a temperature increase which switched off the amplifier due to inner temperature safety devices.
The measured results concerning the answer to a step response showed a higher overshoot than specified. Adjusting the controller parameter to different values in one axis reduced the overshoot but produced an unstable system in other axes.

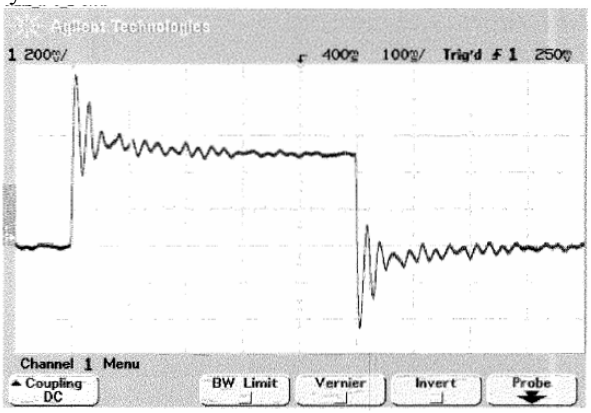

figure 4-1: Step response, z=0, in x, lateral

A frequency plot and a time domain plot of the system in centre position are shown in figure 4-2 and figure 4-1.

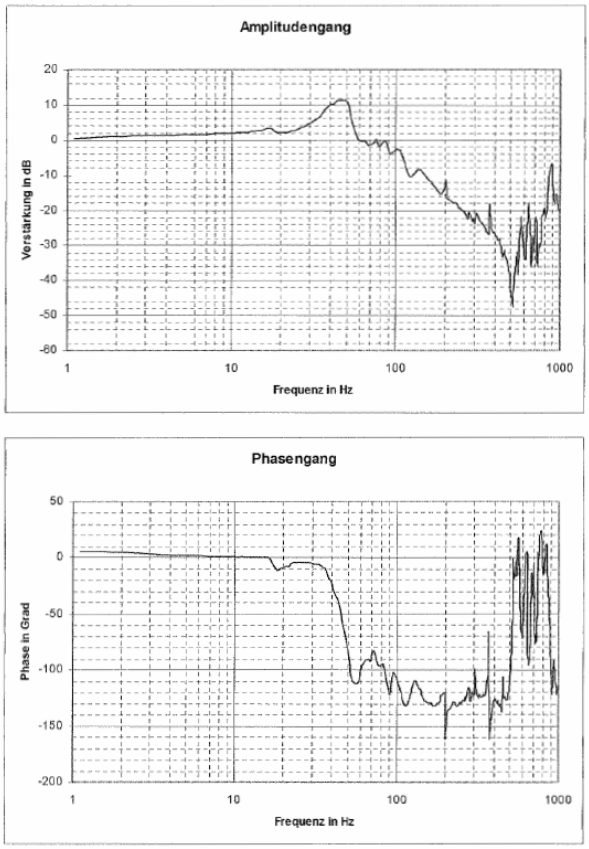

figure 4-2: Bode Plots, z=0, in x, lateral

4.2. Performance Testing

4.2.1. Characterisation

During the set-up the velocity and the position loop for the linear motor was adjusted. Furthermore look-up tables have been created which includes the initial errors which were inverted and fed into the system as correction values.

4.2.2. Functional Performance

During the functional performance test the guidance accuracy has been tested over a stroke of 200 mm.
For the different mirror configuration different look-up tables have been applied. The results for the lateral error in its extreme alignment ranges (x, y) measured with a corner cube mirror are shown in figure 4-3. Included here in the error value is the alignment range of 50 µm and a zero offset error of about 25 µm. The absolute peak error (calculated from x and y deviation) over the stroke of 200 mm is 6 µm which is well in the requirement.

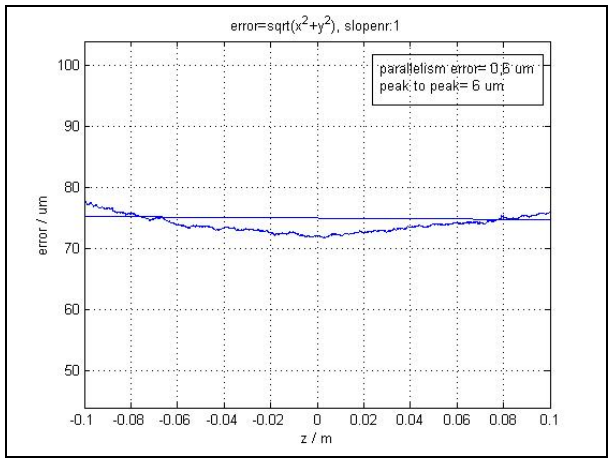

figure 4-3: absolute lateral error

In figure 4-4 the reproducibility over the stroke evaluated from the errors calculated in figure 4-3 is demonstrated. The deviation shows the difference between the first and second scan for the lateral reproducibility in the same direction.

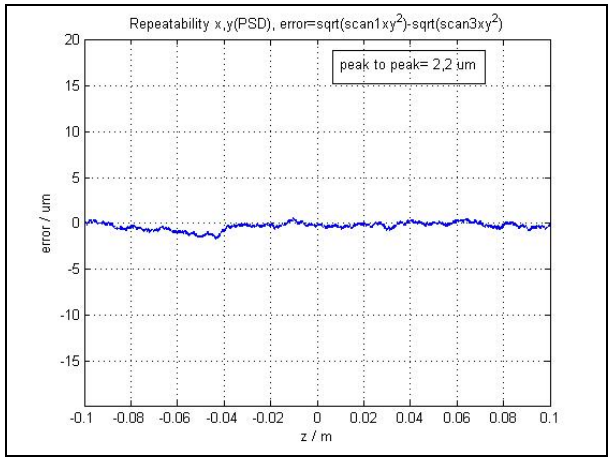

figure 4-4: reproducibility over stroke

The results for the angular error measured with a flat mirror in its extreme alignment ranges (α, β) are shown in figure 4-5. The error here is measured at its extreme alignment range of 100 µrad and an initial offset of about 14 µrad.
The absolute peak to peak error (calculated from α and β deviation) over the stroke of 200 mm is 3.6 µrad which is also in the requirement

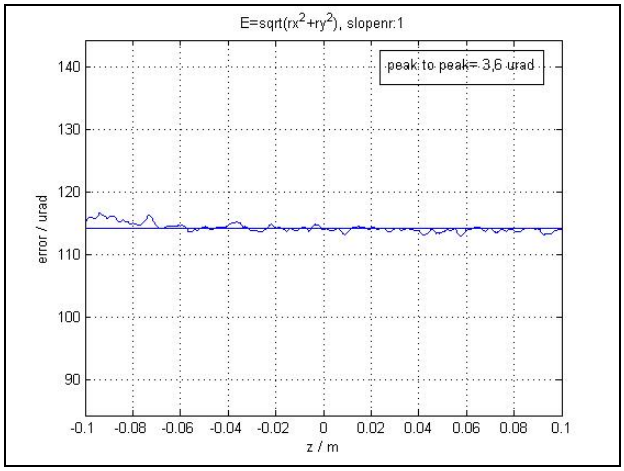

figure 4-5: absolute angular error

In figure 4-6 the reproducibility over the stroke evaluated from the angular errors is demonstrated. The deviation shows the difference between the first and second scan for the angular reproducibility in the same direction. The value is out of specification.

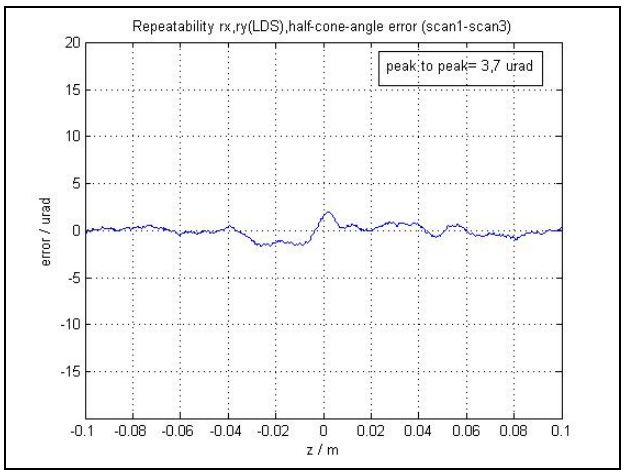

figure 4-6: reproducibility over stroke

The measured performances are shown in figure 4-7 which shows the maximum values in all measured positions:

Requirement	Requ.	Measu.
Linear stroke [mm]	200	> 200
Speed [mm/sec]	25	24,99
Speed stability (RMS) [%]	1	0.02
Guiding Accuracy		
- Mirror tilt max. [µrad]	5.0	3.6 - 11.0
- Tilt reproducibility [µrad]	0.3	2.0 - 5.6
- Lateral deviation [µm]	50	2.2 - 11.0
- Lat. Reproducibility [µm]	3	1.6 - 4.0

figure 4-7: Measured Performances for FTIS

The measured speed stability for 25 mm/sec was well within the required values of less than 1%. figure 4-8 shows the measured speed within the tolerance band of ±1%:

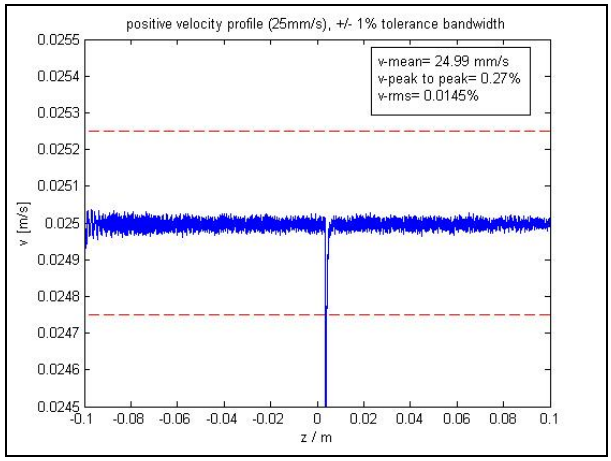

figure 4-8: speed stability

The visible spike was caused to an EMV problem at the encoder reference point but solved later.

4.2.3. Vibration Testing

FTIS has been successfully subjected to sine and random vibration testing. During random vibration testing notches have been applied in order to prevent the rails and the magnetic bearing from touching each other.
The main eigenfrequencies were well above the calculated ones. The applied loads for sine were 20g between 21 and 60 Hz and 6g up to 100 Hz for all axes. The random loads were defined with 0.36 g^2/Hz for out of plane and 0.15 g^2/Hz for the in plane (x, z) axes.
Visual inspection after vibration showed some visible wear at the rear cup/cone connection of the Launch Lock which could be traced back to a bending mode of the sled. The other cup/connections showed the typical behaviour of MoS_2 in changing the colour at the interfacing surfaces.
The release function of the Launch Locking system was not degraded as an functional test showed after vibration testing.

4.2.4. TV Performance

During the thermal vacuum test FTIS also showed an excellent behaviour.
The sensor noise at low temperature (-70°C) slightly increased and the encoder was working although not designed and qualified for the temperature range.

Due to thermal loads and resulting thermal deflections the performance errors were increasing over temperature. Since the errors were of systematic nature they could be compensated by a temperature dependent look-up table.
The performance measurement for the lateral error is shown in figure 4-9 which demonstrates that with the newly created look-up tables at temperature the performance is within the specification.

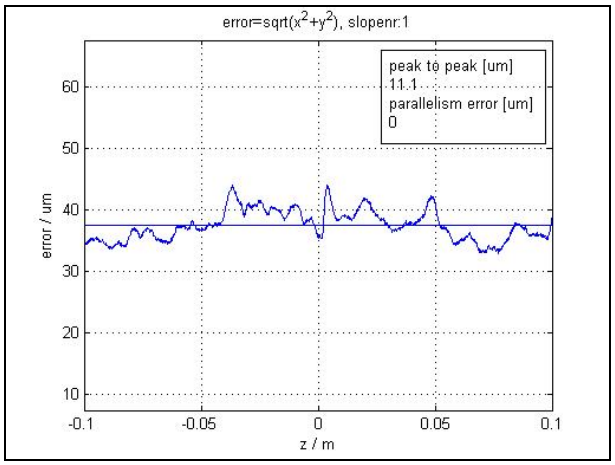

figure 4-9: absolute lateral error under temperature

The reproducibility decreased over temperature which was caused by the set-up of the optical measuring equipment. It has to be taken into account that the static optical error (noise) increased during the temperature test by a factor of 3-4.

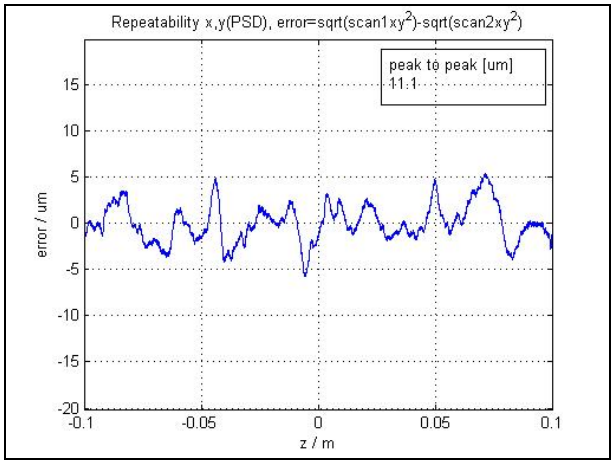

figure 4-10: reproducibility over stroke under temp.

The evaluation of the angular error was not performed due to a run-out of the angular value in y-direction observed during TV-test which is shown in figure 4-11. Several possible cases have been discussed and analysed (bending of base plate, deformation and slipping of magnetic bearings, deformation of sled due to CTE mismatch of the linear motor, etc) indicating thermal-mechanical deformations combined with the sensor scaling but the reason is still unclear. Further analysis and testing is needed in order to identify the source of this run-out.

The repeatability of the angle about y is in the range as during the ambient tests.

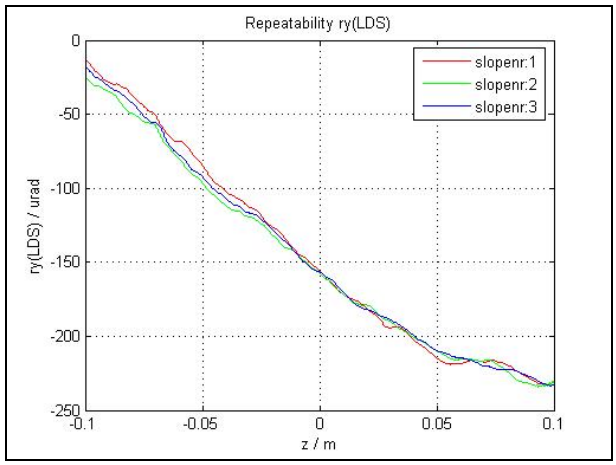

figure 4-11: run-out under temperature

Stability measurements (holding z position) at ambient and under temperature showed excellent results.

5. Design Improvements and Lessons Learnt

Within the project several small design and manufacturing/integration issues occurred. Most of these individual discrepancies were negligible; however taking into account the required extreme performance values in terms of lateral and angular deviations over stroke, the sum of these individual discrepancies was decreasing the overall mechanism performance. In addition a performance decrease was originated by the fact that the development model was not in all aspects flight representative

5.1. FTIS Hardware

The largest error contributors were the mechanical parts and the sensors of FTIS.

- Different behaviour of the bandwidth of the system in its extreme z-positions resulted from the fact that the CoG of the sled was not located in the centre between

the bearings while the sled itself was in centre position (0 position).

- An integration error occurred while gluing the U-coils of the magnets bearings into its housing. Instead of the correct distance of 0.25 mm to the rail the air gap between the rail and one pole of the U-coil was 0.6 mm. A new procedure was developed to avoid such errors in future.
- The position sensors were another contributor to a decrease of performance. The transfer factors of each sensor pair were slightly different from each other which lead to a control lag error in steady state. The transfer factor could not be scaled within the controller hardware. Also the offset could not be adjusted as expected by the supplier.
- The extension of the rails over the sandwich plate caused some stable oscillation at certain frequencies and positions. Not only the whole model should be investigated with a FEM for launch condition - also the sled should be controlled for free oscillation when levitating between the bearings.
- An iso-static mounting between the linear motor and the sled is preferred in order to avoid thermo-elastic effects during temperature changes which cause performance losses.
- High power consumption due to linear amplifier can be reduced by usage of Switched-Mode Power Supply (SMP). This may lead to small decrease in performance

5.2. Optical test set-up

- The optical test set-up was built up with available hardware. Due to the large envelope of the optical measuring device and loss of light due to the absorption of optical elements the initial planned reference mirror could not be installed. This is absolutely necessary if comparable measurements shall be performed.
- Furthermore the static optical jitter produced by the set-up was too large for accurate resolution although the used hardware provided resolution figure about 5 times larger than the minimum required measurement accuracy.

5.3. Testing

- Too much the time has been spent during the development phase to calculate and predict the performance of FTIS by analysis rather than to test the system.
- Much more time should been spent for tests to identify the real performance limits of the H/W and to derive on this basis the improvement potentials in view of a later flight model.

6. Outlook

Despite the fact that the development model is not completely flight representative in terms of materials and processes and also not optimised in view of design, manufacturing and integration, the resulting performance showed very good results.

With all the errors eliminated or decreased to a minimum the performance of this magnetic bearing system can be increased significantly.
The major advantage of this system is that if a performance error concerning the guidance accuracy should occur in orbit, a new look-up table can be created and fed into the system to improve the performance again.

As there is no sliding part no wear or life time issues occur. The lifetime is determined by the controller electronics and the electronics of the linear motor.

Further applications can be envisaged in different scanning mechanism for space applications by implementing appropriate design changes to fit FTIS scan mechanism to a new application.